

Effect of Crosshead Displacement Rates on the Out of Plane Mechanical Properties of S2-Glass Fiber Reinforced Polymers

*Makale Bilgisi / Article Info

Alındı/Received: 09.08.2024

Kabul/Accepted: 12.11.2024

Yayımlandı/Published: xx.xx.xxxx

Test Hızının S2-Cam Elyaf Takviyeli Polimerlerin Düzlem Dışı Mekanik Özelliklerine Etkisi

Çağatay YILMAZ^{1*} , Sara Saeed Abdulrahman ELTAHIR² 

¹ Abdullah Gül University, Faculty of Engineering, Mechanical Engineering, Kayseri, Türkiye

² Abdullah Gül University, Department of Advanced Materials and Nanotechnology, Kayseri, Türkiye



© Afyon Kocatepe Üniversitesi

© 2025 The Authors | Creative Commons Attribution-NonCommercial 4.0 (CC BY-NC) International License

Abstract

Crosshead displacement rates are significant parameters that alter the mechanical response of fiber-reinforced polymeric materials. In this study, we examine the bending behavior of S2-glass fiber-reinforced polymeric materials with different crosshead displacement rates under out-of-plane loading conditions. Out-of-plane loading condition is achieved with a three-point bending fixture. Four different crosshead displacement rates are chosen: 2 mm/min, 20 mm/min, 40 mm/min, and 60 mm/min. Flexural strength, flexural modulus, and flexural strain at maximum load are analyzed. As the crosshead displacement rate increases from 2 mm/min to 20 mm/min and 40 mm/min, both flexural strength and flexural modulus show an upward trend. However, when the crosshead displacement rate increases from 40 mm/min to 60 mm/min, a reduction in the flexural strength and modulus is observed.

Keywords: S2-Glass Fiber; Crosshead Displacement Rates; Composites; Three-Point Bending

Özet

Test hızları, fiber takviyeli polimerik malzemelerin mekanik tepkisini değiştiren önemli parametrelerdir. Bu çalışma kapsamında, düzlem dışı yükleme koşulu altında farklı test hızları ile S2-cam elyaf takviyeli polimerik malzemelerin eğilme davranışlarını incelenmiştir. Düzlem dışı yükleme koşulu üç noktalı eğilme fişkürüyle sağlanmıştır. 2 mm/dk, 20 mm/dk, 40 mm/dk ve 60 mm/dk olmak üzere dört farklı test hızı bu çalışmada kullanılmıştır. Maksimum yükte sehim miktarı, eğilme modülü ve eğilme mukavemeti test hızına bağlı olarak analiz edilmiştir. Test hızı 2 mm/dk'dan 20 mm/dk ve oradan da 40 mm/dk'ya çıktıkça hem eğilme mukavemetinin hem de eğilme modülünün artış eğilimi gösterdiği bulunmuştur. Bununla birlikte, test hızı 40 mm/dk'dan 60 mm/dk'ya yükseldiğinde eğilme mukavemetinde ve modülde bir düşüş gözlemlenmiştir.

Anahtar Kelimeler: S2-Cam Fiber; Test Hızları; Kompozit; Üç Nokta Eğilme

1. Introduction

Glass fiber-reinforced polymeric (GFRP) materials attract the attention of leading industries such as automotive, defense, and wind energy. The reason behind this attraction is the considerably low specific strength and modulus values of GFRP materials. Thanks to the low specific strength and modulus values of GFRP, structural parts can be manufactured with a lower mass, hence enabling less fuel consumption for automobiles providing better solutions for defense and wind energy industries. GFRP materials possess an anisotropic behavior, and this behavior defines the material properties in different axes and planes. Generally, material properties of GFRP are characterized in in-plane. However, out-of-plane mechanical properties also demonstrate a significant level of importance due to the

response of the GFRP materials to an applied load. While an in-plane load is generally carried by the reinforcement, an out-plane load is carried both by the fiber and matrix.

The out-of-plane mechanical test is usually performed under quasi-static conditions in which the crosshead displacement rates are usually between 0,5 and 2 mm/min (Kiyak & Kaman, 2018; Mei et al., 2022; Zniker et al., 2023). However, out-of-plane mechanical properties of GFRP can be dependent on crosshead displacement rates, and experiments need to be performed on the required crosshead displacements for the planned applications. For that purpose, different crosshead displacement rates are used in the literature (Amjadi & Fatemi, 2020; Jemii et al., 2022). It is shown that the transverse compressive strength of

carbon/epoxy laminates increases as the strain rate increases (Hsiao & Daniel, 1998). This increase in the transverse compressive strength is attributed to stiffening of the composite in-plane shear behavior and changing of the failure modes. Tensile properties of long glass fiber-reinforced polypropylene composites under unidirectional tension are examined with different strain rates (Wang et al., 2023). It is shown that as the strain rate increases, tensile strength and tensile fracture stress reveal an upward trend. The effect of strain rates is also studied for the long fiber-reinforced thermoplastic polymer under tensile loading (Cui et al., 2019). It is shown that as the strain rate increases, tensile strength and fracture strain show a rising trend, however, tensile stiffness remains the same. It is documented that the interfacial bonding properties of long-fiber reinforced polymer improves as the strain rate increases. The improvement in the interfacial bonding properties causes a gradual decrease in fiber pull-out. E-glass fiber-reinforced polypropylene composite is tested under off-axis tensile loading, and it is presented that as the strain rate increases, damage initiation in the matrix is postponed (Zhai et al., 2018a). The effect of strain rate on the commingled E-glass/polypropylene woven fabric composite under the tensile, compression, and shear load is examined. It is found that as the strain rate increases, tensile strength, tensile modulus, compression strength, and compression modulus show an upward trend. On the other hand, shear strength and modulus demonstrate a downward trend as the strain rate increases (Brown et al., 2010a). The compressive behavior of woven glass fiber reinforced polymer is analyzed in the in-plane loading direction by considering different strain rates. It is shown that as the strain rate increases a rise in strength and modulus is observed.

However, when the strain rate further increases, a reduction in the strength and modulus is documented. (Shah Khan et al., 2000).

Although a significant number of research in the literature focuses on the effect of crosshead displacement rates of fiber-reinforced polymeric materials under the tensile, compression and shear loading conditions, it is best of the authors' knowledge, there is no study on the effect of crosshead displacements rates to S2-glass fiber reinforced polymeric materials under the out of plane loading conditions. Therefore, S2-glass fiber reinforced polymer produced with the vacuum infusion method is used as a material under study. Samples are grouped into four and labeled as groups A, B, C, and D. These four groups are tested with a testing speed of 20 mm/min, 40 mm/min, 60 mm/min, and 2 mm/min by using a three-point bending fixture to examine the effect of testing speed on the out of plane strength, modulus and strain of S2-glass fiber reinforced polymer.

2. Materials and Methods

2.1 Materials and sample preparation

S2-glass-fiber plain-weave fabrics with an aerial weight of 800 gsm is used as a reinforcement. As a matrix material, Biresin CR 122 epoxy and Biresin CH122-5 are used. The composite plate is manufactured with a vacuum infusion method. First, the heated plate is cleaned with acetone. Four layers of releasing agent are applied to the heated plate to prevent sticking of the produced composite plate to the heated table. Four layers of S2-glass fabrics are layered on the heated plate. Vacuum infusion consumables, as seen in Figure 1, are placed over the S2-glass fabric.

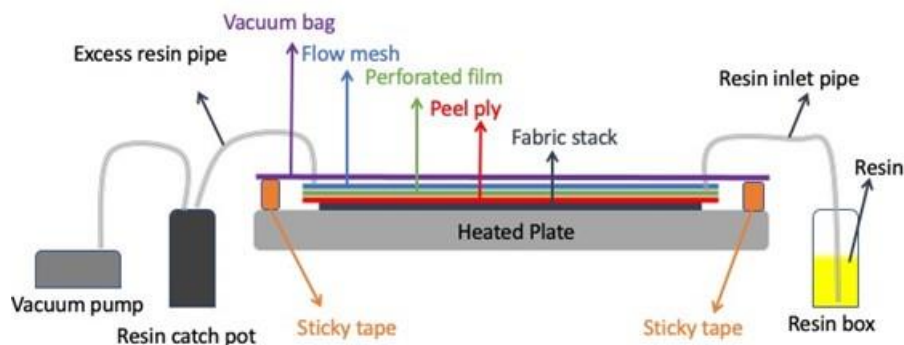


Figure 1: Schematic of the vacuum-infusion process and order of consumables used in the production of the composite test plate

First, a peel ply, then a perforated film, and flow mesh followed by a vacuum bag is spread out on four layers of S2-glass fabrics in turn. A double-sided vacuum tape is put on the perimeter of four S2-glass layers. Thereafter, the vacuum bag is adhered to double-sided tape to seal

the four layers of S2-glass fiber from the open atmosphere. Once the bagging is completed, a leak check procedure is followed to ensure air tightness of the vacuum infusion setup. The whole setup is vacuumed, and the level of vacuum on the gauge is

recorded. Both the inlet and outlet of the whole set-up is blocked, and it is left for 10 minutes while the vacuum pump is on. After 10 minutes, the airflow in the outlet is ensured and no drop in the vacuum gauge is observed. Then epoxy resin is mixed with hardener with a weight ratio of 100:30. Thereafter, the mixture is degassed for 10 minutes to remove the entrapped air bubbles introduced to the resin-hardener mixture during mechanical stirring. S2-glass fabric stack is impregnated by the resin mixture and then followed by a curing at 90 °C for 18 hours. Curing is completed on a heated plate. The produced plate is cut into test coupons as per the dimensions given in ASTM D790 by using a three-axis CNC milling machine.

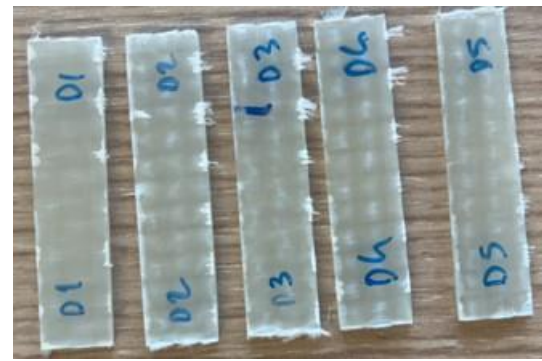
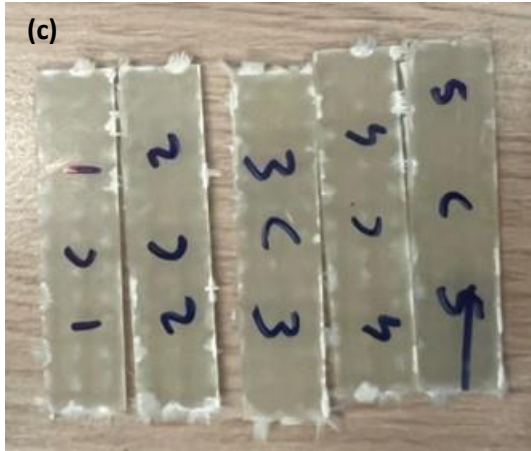
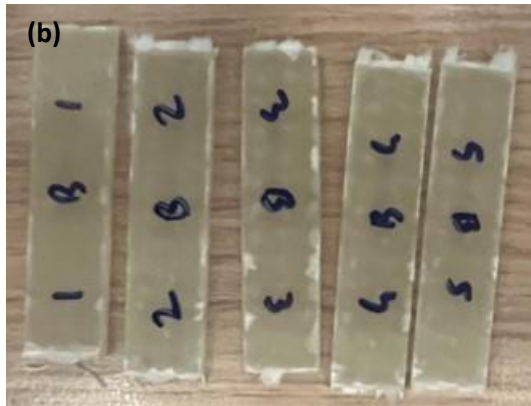
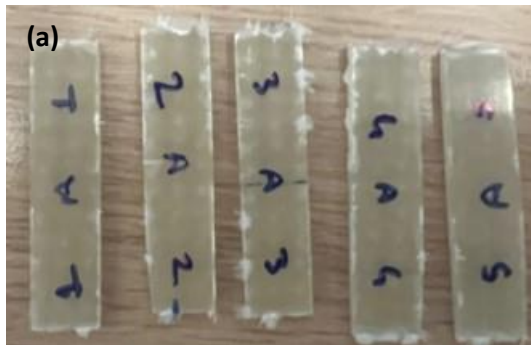


Figure 2: Specimens just before the 3-point bending test



(d)

The samples that are prepared for the 3-point bending test can be seen in Figure 2. Samples are grouped into four, namely A, B, C, and D, and tested with different strain rates.

2.2 Mechanical testing

The three-point testing is performed with a Shimadzu AGS-X UTM (Universal Testing Machine) machine equipped with a load cell of 10 kN to measure the out-of-plane mechanical properties of the produced test coupons. Sample dimensions are chosen as per the ASTM D 790 standard. Average sample thickness, width, support span, and sample length are 2.75 mm, 12.75 mm, 44 mm, and 60 mm, respectively. According to ASTM D790 standard, a crosshead displacement of 2 mm/min can be used, for the given sample dimensions, 2 mm/min corresponds to a strain rate of 0.00028 s^{-1} . To investigate the effect of higher strain rates on the out-of-plane mechanical properties of S2-glass fiber-reinforced polymeric materials, different crosshead displacement rates are employed. Group A is tested with a crosshead displacement of 20 mm/min, which corresponds to a strain rate of 0.0028 s^{-1} . That strain rate is tenfold that suggested in the ASTM D 790 standard. Groups B and C are tested with a crosshead displacement of 40 mm/min and 60 mm/min. These crosshead displacements correspond to a strain rate of 0.0056 s^{-1} and 0.0084 s^{-1} , respectively. Group D is tested with a crosshead displacement of 2 mm/min as a control group. For each crosshead displacement, five specimens are tested to get an average result and standard deviation of flexural strength, flexural modulus, and flexural strain. A photo from the 3-point bending test can be seen in Figure 3.

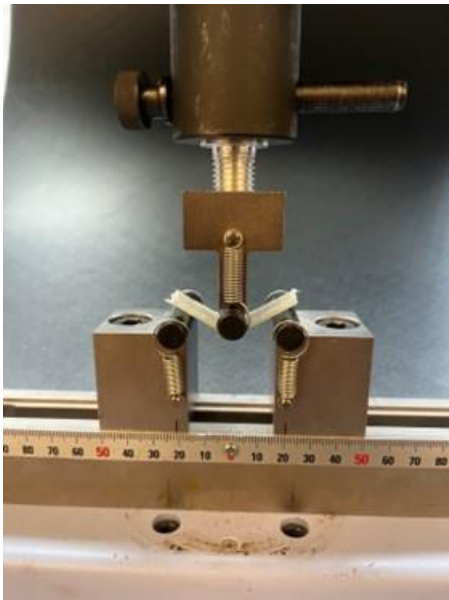


Figure 3: A sample tested with a 3-point bending fixture

3. Results and Discussions

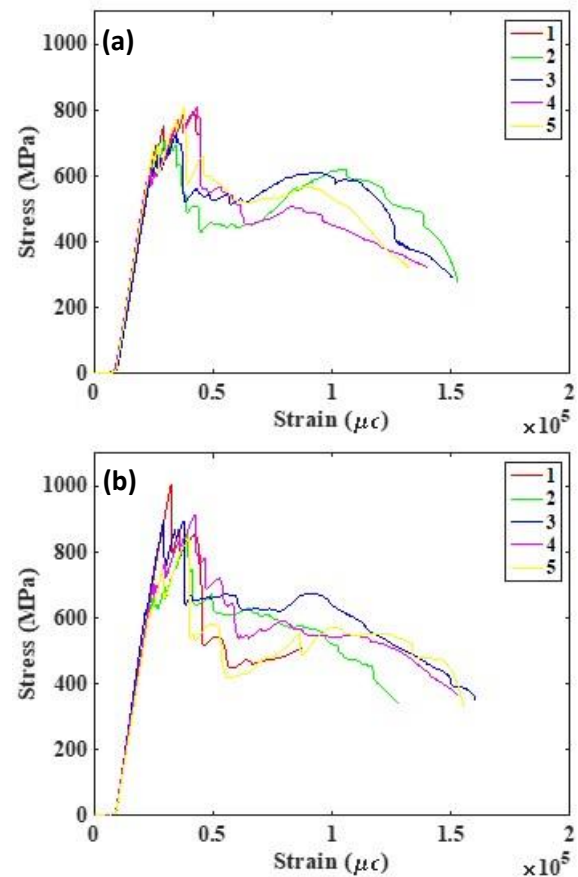
This study is designed to examine the effect of crosshead displacement rates on the out-of-plane mechanical properties of S2-glass fiber-reinforced thermoset polymer. Four crosshead displacement rates, 2mm/min, 20 mm/min, 40 mm/min, and 60 mm/min, are chosen for this study. Samples with tested under 20 mm/min, 40 mm/min, 60 mm/min, and 2 mm/min are marked as batch A, B, C, and D respectively.

As it is discussed in the previous section, these crosshead displacements rates correspond to strain rate of $0.0028 s^{-1}$, $0.0056 s^{-1}$, $0.0084 s^{-1}$, and $0.00028 s^{-1}$, respectively. These strain rates are tenfold, twentyfold, and thirtyfold of the strain rate suggested in ASTM D790 for the given sample dimensions. Stress-strain graph of batches A, B, C, and D can be seen in Figure 4 (a), (b) (c), and (d) respectively.

From the stress-strain graph of each batch, it can be concluded that specimens follow the same path, and failure occurs around $1.5 \times 10^5 \mu\epsilon$. The initial portion of the plot indicates a linear stress-strain curve. Once the critical load is achieved for the first ply failure, the stress-strain curve follows a zigzag pattern, which is an indication of the failure of the other plies. Once the stress-strain graph of each sample achieves a maximum stress level, there is a sudden drop in the stress. This sudden drop indicates that all the plies that consist of composite laminate are damaged. However, a complete failure is not observed after the maximum stress level in the stress-strain curves of all samples.

The effect of crosshead displacement rates on the flexural strength, flexural modulus, and strain at the maximum stress are tabulated in Table 1. It can be deduced from Table 1 that as the crosshead displacement rate increases from 2 mm/min to 20 mm/min and 40 mm/min, flexural strength increases from 646 MPa to 760 MPa and then 900 MPa, which is equal to a rise of 17.6% for the first case and for the latter 18 % in the flexural strength. When the displacement rate rises from 40 mm/min to 60 mm/min, flexural strength decreases from 900 MPa to 810 MPa, which corresponds to a reduction of 10 % in the flexural strength.

The behavior of increasing strength as the strain rate increases and decreasing strength as the strain rate continues to increase is also observed in another study (Weng et al., 2021) and attributed to changes in the failure modes as the strain rate increases. The same behavior is also observed for the flexural modulus.



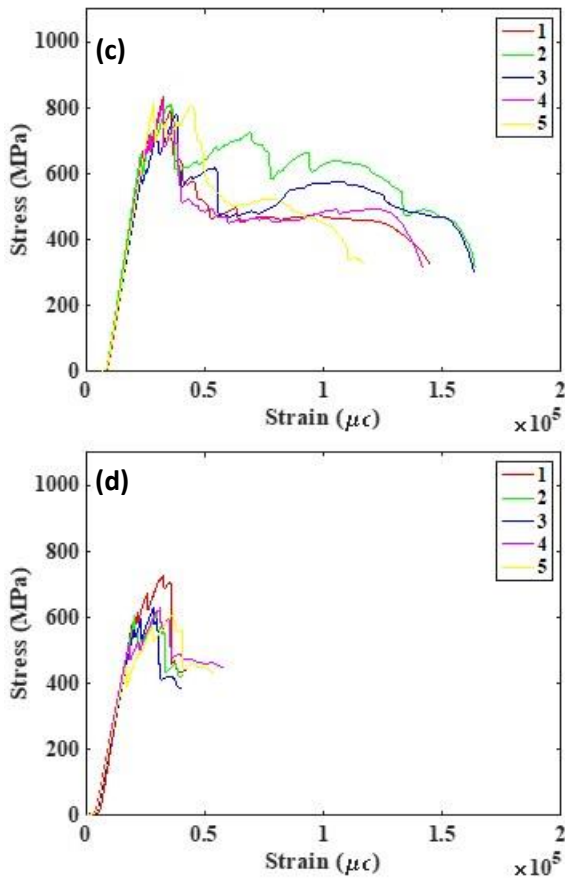


Figure 4: Stress-strain plot of samples, a) tested in 20 mm/min (Group A), b) tested in 40 mm/min (Group B), c) tested in 60 mm/min (Group C), d) tested in 2 mm/min (Group D)

First, a rise and then a drop in the flexural modulus of S2-glass fiber-reinforced polymeric materials is observed with an increase in the crosshead displacement rates. Flexural strain at maximum stress does not show a significant difference concerning increasing crosshead displacement rates.

Table 1: Flexural properties of S2-glassfiber reinforced polymer

Property	Batch A	Batch B	Batch C	Batch D
Flexural Strength (MPa)	760.8 (±49.05)	900 (±74.13)	810.26 (±22.5)	646 (±53.97)
Flexural Modulus (GPa)	42.4 (±1.58)	45.5 (±2.46)	42.96 (±2.31)	37.5 (± 3.3)
Flexural Strain at maximum stress (μϵ)	35135 (±3924)	35158 (±5084)	33731 (±4069)	32076 (±3654)

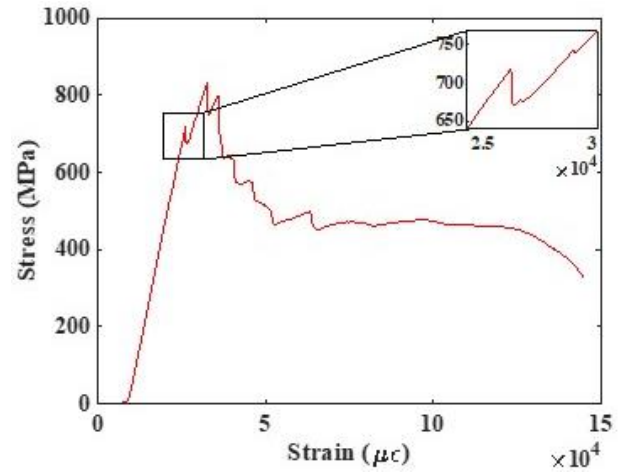


Figure 5: Observation of first ply failure point from the stress-strain curve of the tested sample

The first ply failure response of S2-glass fiber reinforced polymeric material is also analyzed by checking the first ply failure point from the stress-strain curve of each sample. Figure 5 shows the stress-strain curve of a representative specimen with a zoomed portion indicating the first ply failure point. The first ply failure strength and strain of each batch with a standard deviation can be seen in Figure 6. The low standard deviation bars both in Figure 6 (a) and (b) for the strain and stress level of first ply failure indicates that results obtained are scattered over a small range. The small scatter range is a good indicator of the reliability of the test. As the crosshead displacement rate increases, there is a constant rise in the first ply failure stress and strain of S2-glass fiber-reinforced polymeric material. The underlying reason behind this phenomenon is the strain rate dependency of tested material. Such strain rate dependency behavior is also documented elsewhere (Li et al., 2016; Shah Khan et al., 2000). This increase in literature is explained by the occurrence of different damage modes for different strain rates along with the viscoelastic property of both reinforcement and matrix (Barre et al., 1996). Fibre-matrix interface and woven reinforcement pattern is also being kept responsible from this behavior (Brown et al., 2010b).

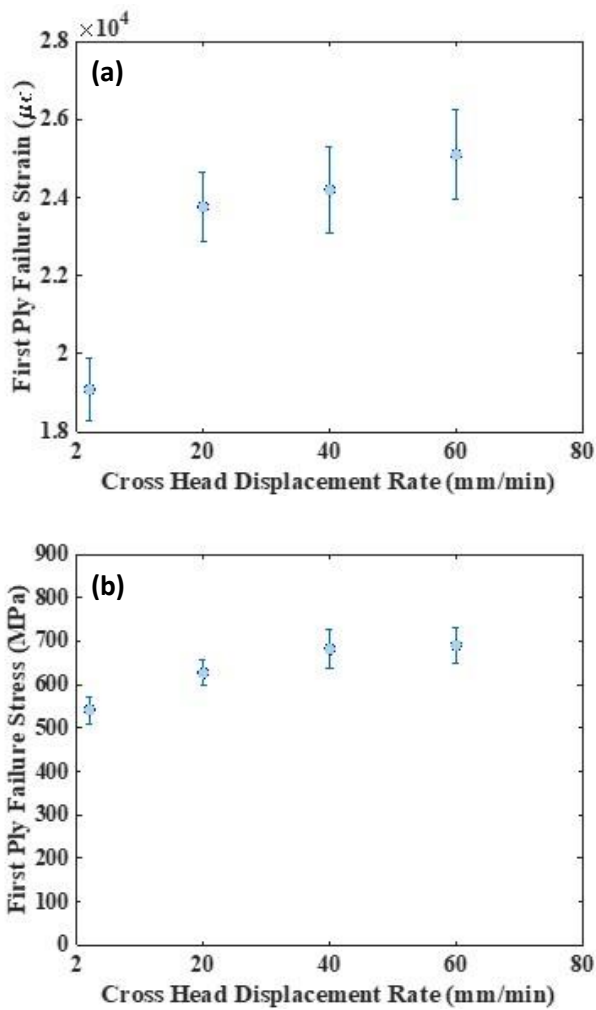


Figure 6: First ply failure, a) Strain, b) Stress

Samples after the three-point bending test can also be seen in Figure 7. Although all samples are still intact, they indicate a severe damage state. When the samples surfaces are analyzed, a severe delamination can be seen in Figure 7.

A lateral view of tested samples is given in Figure 8 to give a more comprehensive view of the damage mechanism. The sample from group D indicates less deformation when compared with other samples from groups A, B, and C. It is clear that samples from groups A, B, and C imply severe delamination, fiber rupture, and a deviation in the plane of the fabric layers due to the failure. Failed representative specimen from group A bespeaks more deformation than that of groups B and C. This result is the confirmation of the change of damage modes as the strain rate increases. The change in the damage modes as the strain rate increases is also observed in previous studies (Perry & Walley, 2022; Zhai et al., 2018b).

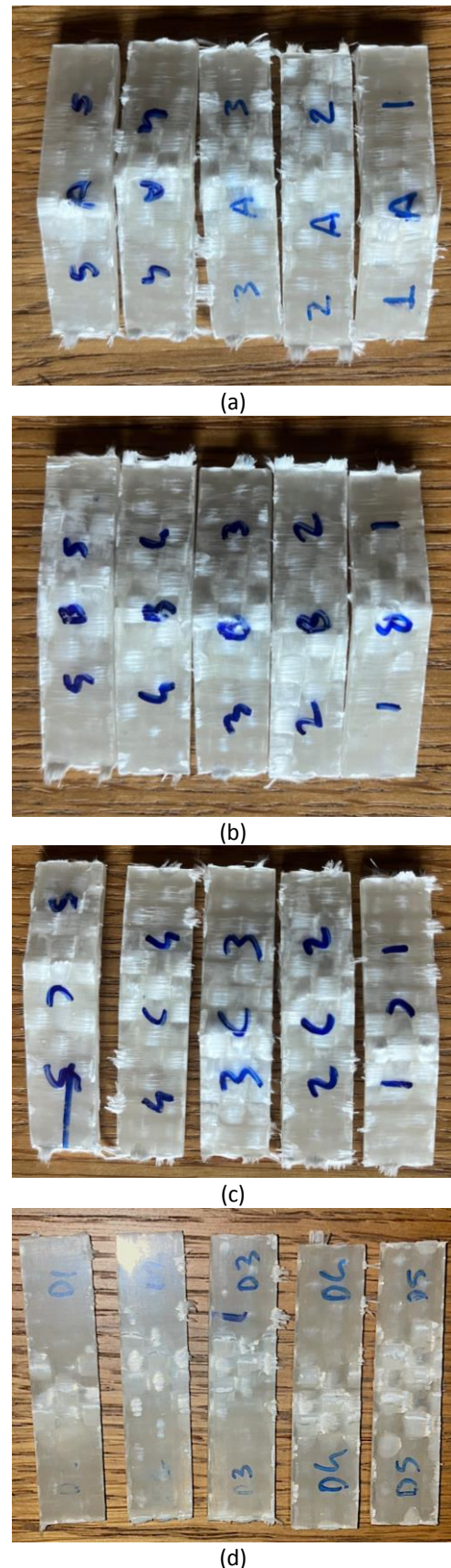


Figure 7: Test specimens, a) Batch A, b) Batch B, c) Batch C, d) Batch D



Figure 8: Lateral view of test representative specimens from each group

4. Conclusions

Herein, we applied different crosshead displacement rates to show the out-of-plane mechanical behavior of S2-glass fiber-reinforced polymeric materials. 2 mm/min, 20mm/min, 40 mm/min, and 60 mm/min are applied as crosshead displacement rates. Out-of-plane stress state is applied with a three-point bending fixture. The effect of displacement rates is analyzed by considering the change in flexural strength, flexural modulus, and strain at maximum load. The effect of crosshead displacement on the damage onset of the S2-glass fiber-reinforced polymeric material is also investigated by calculating first-ply failure stress and strain. Conclusions given below are drawn from this study:

1) It is seen that as the crosshead displacement rates increase from 2 mm/min to 20 mm/min, and then 40 mm/min, both flexural strength and flexural modulus increase. When crosshead displacement rates rise from 40 mm/min to 60 mm/min, a drop in both flexural strength and modulus is observed.

2) Flexural strain at maximum stress does not demonstrate a comparable change when the crosshead displacement rate rises from 20 mm/min to 40 mm/min. However, when the crosshead displacement increases from 40 mm/min to 60 mm/min, a small reduction in the flexural strain at maximum stress occurs.

3) Damage onset is studied by considering the first ply failure analysis. It is shown that as the crosshead displacement rate increases, the required stress and strain level to damage the first ply also rises.

Declaration of Ethical Standards

The authors declare that they comply with all ethical standards.

Credit Authorship Contribution Statement

Author 1: Conceptualization, Methodology / Study design Validation, Formal analysis, Investigation, Resources, Data curation, Writing – original draft, Writing – review and editing, Visualization, Supervision, Project administration, Funding acquisition

Author 2: Conceptualization, Validation, Formal analysis, Investigation, Resources, Data curation, Writing – original draft, Writing – review and editing

Declaration of Competing Interest

The authors have no conflicts of interest to declare regarding the content of this article.

Data Availability

All data generated or analyzed during this study are included in this published paper.

Acknowledgment

The authors gratefully acknowledge support from the Scientific and Technological Research Council of Turkey (TUBITAK) under grant number 221M085.

5. References

- Amjadi, M., & Fatemi, A. (2020). Tensile behavior of high-density polyethylene including the effects of processing technique, thickness, temperature, and strain rate. In *Polymers*, **12(9)**, 1857-1870
<https://doi.org/10.3390/polym12091857>
- Barre, S., Chotard, T., & Benzeggagh, M. L. (1996). Comparative study of strain rate effects on mechanical properties of glass fibre-reinforced thermoset matrix composite. *Composites Part A: Applied Science and Manufacturing*, **27(12)**, 1169–1181.
[https://doi.org/10.1016/1359-835X\(96\)00075-9](https://doi.org/10.1016/1359-835X(96)00075-9)
- Brown, K. A., Brooks, R., & Warrior, N. A. (2010a). The static and high strain rate behaviour of a commingled E-glass/polypropylene woven fabric composite. *Composites Science and Technology*, **70(2)**, 272–283.
<https://doi.org/10.1016/j.compscitech.2009.10.018>
- Brown, K. A., Brooks, R., & Warrior, N. A. (2010b). The static and high strain rate behaviour of a commingled E-glass/polypropylene woven fabric composite. *Composites Science and Technology*, **70(2)**, 272–283.
- Cui, J., Wang, S., Wang, S., Li, G., Wang, P., & Liang, C. (2019). The effects of strain rates on mechanical properties and failure behavior of long glass fiber reinforced thermoplastic composites. *Polymers*, **11(12)**, 2019-2036
<https://doi.org/10.3390/polym11122019>
- Hsiao, H. M., & Daniel, I. M. (1998). Strain rate behavior of composite materials. *Composites Part B: Engineering*, **29(5)**, 521–533.
[https://doi.org/10.1016/S1359-8368\(98\)00008-0](https://doi.org/10.1016/S1359-8368(98)00008-0)
- Jemii, H., Bahri, A., Taktak, R., Guerhazi, N., & Lebon, F. (2022). Mechanical behavior and fracture characteristics of polymeric pipes under curved three point bending tests: Experimental and numerical approaches. *Engineering Failure Analysis*, **138**, 106352.
<https://doi.org/10.1016/j.engfailanal.2022.106352>

- Kiyak, B., & Kaman, M. O. (2018). Karbon fiber kompozit sandviç levhaların yanal mukavemet davranışlarının araştırılması. *Afyon Kocatepe Üniversitesi Fen ve Mühendislik Bilimleri Dergisi*, **18(2)**, 684–691.
<https://doi.org/10.5578/fmbd.67199>
- Li, X., Yan, Y., Guo, L., & Xu, C. (2016). Effect of strain rate on the mechanical properties of carbon/epoxy composites under quasi-static and dynamic loadings. *Polymer Testing*, **52**, 254–264.
<https://doi.org/10.1016/j.polymertesting.2016.05.002>
- Mei, J., Liu, J., & Huang, W. (2022). Three-point bending behaviors of the foam-filled CFRP X-core sandwich panel: Experimental investigation and analytical modelling. *Composite Structures*, **284**, 115206.
<https://doi.org/10.1016/j.compstruct.2022.115206>
- Perry, J. I., & Walley, S. M. (2022). Measuring the effect of strain rate on deformation and damage in fibre-reinforced composites: A Review. *Journal of Dynamic Behavior of Materials*, **8(2)**, 178–213.
<https://doi.org/10.1007/s40870-022-00331-0>
- Shah Khan, M. Z., Simpson, G., & Gellert, E. P. (2000). Resistance of glass-fibre reinforced polymer composites to increasing compressive strain rates and loading rates. *Composites Part A: Applied Science and Manufacturing*, **31(1)**, 57–67.
[https://doi.org/10.1016/S1359-835X\(99\)00051-2](https://doi.org/10.1016/S1359-835X(99)00051-2)
- Wang, Q., Wang, J., Wang, A., Zhou, C., Hu, J., & Pan, F. (2023). Effect of strain rate and temperature on the tensile properties of long glass fiber-reinforced polypropylene composites. In *Polymers*, **15(15)**, 3260
<https://doi.org/10.3390/polym15153260>
- Weng, F., Fang, Y., Ren, M., Sun, J., & Feng, L. (2021). Effect of high strain rate on shear properties of carbon fiber reinforced composites. *Composites Science and Technology*, **203**, 108599.
<https://doi.org/10.1016/j.compscitech.2020.108599>
- Zhai, Z., Jiang, B., & Drummer, D. (2018a). Strain rate-dependent mechanical behavior of quasi-unidirectional E-glass fabric reinforced polypropylene composites under off-axis tensile loading. *Polymer Testing*, **69**, 276–285.
<https://doi.org/10.1016/j.polymertesting.2018.05.033>
- Zniker, H., Feddal, I., Ouaki, B., & Bouzakraoui, S. (2023). Experimental and numerical investigation of mechanical behavior and failure mechanisms of pvc foam sandwich and grp laminated composites under three-point bending loading. *Journal of Failure Analysis and Prevention*, **23(1)**, 66–78.
<https://doi.org/10.1007/s11668-023-01596-w>